

Endothelial Cell Indoleamine 2, 3-Dioxygenase 1 Alters Cardiac Function Following Myocardial Infarction Through Kynurenine

Running Title: *Melhem et al.; Tryptophan Catabolism in Myocardial Infarction*

Nada Joe Melhem, et al.

The full author list is available on page 21.

Address for Correspondence:

Soraya Taleb, PhD

PARCC-INSERM U970

56 rue Leblanc, 75015 Paris, France

Email: soraya.taleb@inserm.fr



This article is published in its accepted form, it has not been copyedited and has not appeared in an issue of the journal. Preparation for inclusion in an issue of <journal name> involves copyediting, typesetting, proofreading, and author review, which may lead to differences between this accepted version of the manuscript and the final, published version.

Abstract

Background: Ischemic cardiovascular diseases, particularly acute myocardial infarction (MI) is one of the leading cause of mortality worldwide. Indoleamine 2, 3-dioxygenase 1 (IDO) catalyzes one rate-limiting step of L-Tryptophan (Trp) metabolism, and emerges as an important regulator of many pathological conditions. We hypothesized that IDO could play a key role to locally regulate cardiac homeostasis after MI.

Methods: Cardiac repair was analyzed in mice harboring specific endothelial or smooth muscle cells or cardiomyocyte or myeloid cell deficiency of IDO and challenged with acute myocardial infarction.

Results: We show that Kynurenine (Kyn) generation through IDO is markedly induced after MI in mice. Total genetic deletion or pharmacological inhibition of IDO limits cardiac injury and cardiac dysfunction after MI. Distinct loss of function of IDO in smooth muscle cells, inflammatory cells, or cardiomyocytes does not impact cardiac function and remodeling in infarcted mice. In sharp contrast, mice harboring endothelial cell-specific deletion of IDO show an improvement of cardiac function, as well as cardiomyocyte contractility and reduction in adverse ventricular remodeling. *In vivo* Kyn supplementation in IDO-deficient mice abrogates the protective effects of IDO deletion. Notably, Kyn precipitates cardiomyocyte apoptosis through reactive oxygen species production in an aryl hydrocarbon receptor-dependent mechanism.

Conclusions: These data suggest that IDO could constitute a new therapeutic target during acute MI.

Key Words: Tryptophan; Kynurenine; IDO; apoptosis; myocardial infarction

Non-standard Abbreviations and Acronyms

AA: Anthranilic acid
 AHR: Aryl Hydrocarbon Receptor
 BM: Bone Marrow
 CM: Cardiomyocyte
 CEEA : Comité d'Ethique en Experimentation Animale
 DHE: Dihydroethidium
 EC: Endothelial Cell
 EF: Ejection Fraction
 FITC: Fluorescein isothiocyanate
 3-HAA: 3-Hydroxyanthranilic acid
 HR: Heart rate
 IDO: Indoleamine 2, 3-dioxygenase 1
 IFN- γ : Interferon-gamma
 IL: Interleukin
 Kna: Kynurenic acid
 Kyn: Kynurenine
 LPS: Lipopolysaccharide
 LV: Left Ventricle
 L-1MT: 1-Methyl-L-tryptophan
 MI: Myocardial Infarction

Myh6: α -Myosin heavy chain
 3-OHKyn: 3-Hydroxykynurenine
 PE: Phycoerythrin
 Quina: Quinolinic acid
 ROS: Reactive Oxygen Species
 SL: Sarcomere Length
 SMC: Smooth Muscle Cell
 TNF- α : Tumor Necrosis Factor- α
 Tregs: Regulatory T cells
 Trp: Tryptophan
 TUNEL: Terminal deoxynucleotidyl transferase dUTP nick-end labeling
 Vd: LV end-diastolic volume
 Vs: LV end-systolic volume
 WT: Wild-type

Clinical Perspective

What is new?

- Indoleamine 2, 3-dioxygenase 1 (IDO), an enzyme involved in Tryptophan catabolism, precipitates adverse cardiac remodeling after acute myocardial infarction.
- The specific deletion of IDO in endothelial cells enhances cardiomyocyte survival and contractility leading to cardiac function improvement.
- IDO dependent effects are mediated by endothelial cell production of kynurenine.

What are the clinical implications?

- Our study provides novel insights into the complex cross-talk between the cardiac endothelial cells and cardiomyocytes during cardiac repair after myocardial infarction and suggests a deleterious role for endothelial IDO through kynurenine production in cardiac repair.
- Therapeutic strategy targeting cardiac IDO could constitute an innovative approach to curb cardiac dysfunction following acute myocardial infarction.

Introduction

Myocardial infarction (MI), by promoting adverse remodeling of the left ventricle (LV), is a leading cause of morbidity and mortality worldwide. Following MI, intricate interactions among different cellular entities such as cardiomyocytes (CM), inflammatory and vascular cells are instrumental in the regulation of tissue remodeling and govern the prevalence of heart failure, arrhythmias, or sudden death¹. Therefore, it is of great importance to unravel the mechanisms underlying adverse cardiac remodeling and subsequently to explore new therapeutic approaches in patients with MI.

Indoleamine 2, 3-dioxygenase 1 (IDO) is an enzyme that catalyzes the degradation of the essential amino acid L-tryptophan (Trp) to N-formylkynurenine leading to the generation of several active metabolites including kynurenine (Kyn), 3-hydroxykynurenine (3-OHKyn), anthranilic acid (AA), 3-hydroxyanthranilic acid (3-HAA), kynurenic acid (Kna) and quinolinic acid (Quina). IDO-related pathways have been involved in various diseases ranging from chronic granulomatous disease² to neurodegenerative diseases³, and more recently in cardiometabolic diseases including metabolic syndrome⁴, aneurysm^{5, 6} and atherosclerosis⁷⁻¹¹. In these experimental models, either protective^{4-6, 11} or deleterious⁷⁻¹⁰ effects of IDO-generated metabolites have been reported. Yet, in human studies, IDO activity was constantly found to be associated with worse cardiovascular outcome in patients with coronary artery disease¹²⁻¹⁴ and atherosclerosis progression in patients with end-stage renal disease¹⁵.

During inflammation, IDO is up-regulated mostly in dendritic cells and macrophages by pro-inflammatory stimuli such as tumor necrosis factor- α (TNF- α), interleukin-6 (IL-6)¹⁶, and interferon-gamma (IFN- γ)¹⁷. IDO exerts its biological effects through the generation of downstream metabolites that suppress effector T-cell function and favor the differentiation of

regulatory T cells (Tregs)¹⁸. However, the biological effects of IDO extend beyond its role in the regulation of the immune response. Interestingly, IDO activity has been shown to contribute to arterial vessel relaxation and regulation of blood pressure in septic shock¹⁹, and to promote renal ischemia-reperfusion injury²⁰. Recent studies have also demonstrated that Kyn metabolites may increase inflammation²¹, oxidative stress, as well as apoptosis of smooth muscle and endothelial cells (EC)^{6, 22}.

Given the potential link between IDO-dependent pathways and MI, we hypothesized that IDO activity is induced after acute MI and is instrumental in the regulation of cardiac remodeling and function. Here, we show that, deficiency or pharmacological inhibition of IDO protects against MI-induced cardiac dysfunction. Moreover, conditional loss of function of IDO in EC, but not in smooth muscle cells (SMC), or in CM or in bone marrow (BM)-derived inflammatory cells, reduces infarct size and limits cardiac injury after MI. Furthermore, we demonstrate that Kyn is responsible for the deleterious effects observed in IDO-deficient mice. Collectively, our results reveal the biological importance of Kyn produced by EC in the context of ischemic cardiac injury. These findings could have implications for the development of novel therapeutic strategies aimed at inhibiting IDO activity for the treatment of patients with ischemic cardiac diseases.

Methods

The data, analytic methods, and study are available from the corresponding author on reasonable request.

Animals

Ido1^{-/-} mice were from the Jackson Laboratory and are raised in our facility. CM deficiency was achieved by crossbreeding transgenic B6129-Tg (*Myh6-cre/Esr1*)1Jmk/J, in which the CM-specific α -myosin heavy chain (*Myh6*) promoter drives expression of a 4-OH-tamoxifen inducible Cre recombinase fusion protein with *Ido-1*^{flox/flox} mice (*Ido-1*^{flox/flox} α MHC-Cre). SMC deficiency was achieved by crossbreeding transgenic B6.Cg-Tg(*Tagln-cre*)1Her/J, in which the mouse smooth muscle protein 22-alpha promoter drives expression of a Cre recombinase with *Ido-1*^{flox/flox} (*Ido-1*^{flox/flox} SM22-Cre). EC deficiency was obtained by crossbreeding transgenic Tg (*Cdh5-cre/ERT2*⁺), in which the vascular EC-specific cadherin promoter drives expression of a tamoxifen inducible Cre recombinase with *Ido-1*^{flox/flox} mice (*Ido-1*^{flox/flox} VECad-CreERT2⁺). In both CM and EC deficiency, the Cre-mediated excision of floxed *Ido-1* alleles was induced by treatment with Tamoxifen containing diet (Harlan) for 15 days. *Ido1*^{-/-}, *Ido-1*^{flox/flox} α MHC-Cre (CM IDOKO), *Ido-1*^{flox/flox} SM22-Cre (SMC IDOKO) and *Ido-1*^{flox/flox} VECad-CreERT2 (EC IDOKO) mice and their respective littermate controls (*Ido1*^{+/+}, CM IDO, SMC IDO and EC IDO) were on a C57Bl/6J background. All experiments were performed in 10- to 12-week-old male animals, because of their higher susceptibility to MI compared to females²³. In some experiments, wild-type (WT) mice were treated with the IDO inhibitor, 1-Methyl-L-tryptophan (L-1MT, 2mg/mL in drinking water), during 4 weeks before ligature and then 14 days after MI until sacrifice. Other *Ido1*^{-/-} mice were supplemented with Kyn (2mg/mL in drinking water), and some of these mice were injected with Aryl Hydrocarbon Receptor (AHR) antagonist CH-223191 (100 μ g/mouse) or its vehicle, 3 times during 1 week before MI. Some WT and *Ido1*^{-/-} mice were also subjected to medullar aplasia by 9.5 gray lethal total body irradiation and were repopulated 24 hours later with an intravenous injection of 1 \times 10⁷ total BM cells isolated from

femurs and tibias of age- and sex-matched WT and *Ido1*^{-/-} mice. Mice were then challenged with MI 4 weeks after BM reconstitution. Sample size has not been predetermined by statistical method. Adult mice dying within 24 hours of coronary artery ligation surgery (<10% in all genotypes studied) were prespecified as purely technical failures and excluded from subsequent analysis. Experiments were conducted according to the French and European community guidelines for experimental animal use and to the institutional guidelines approved by the local ethics committee of the French authorities, the 'Comité d'Ethique en Experimentation Animale' (CEEA) under the following number 01373.03. All the animals were maintained under identical standard conditions including housing, regular care, and normal chow in the same animal facility throughout the duration of the experiments.

Myocardial Infarction




MI was induced by left coronary ligation as previously described²⁴. The exact same procedure was performed for the sham-operated mice except that the ligation was not tied. All MI experiments were performed in a blinded manner with regard to the genotype of mice.

Echocardiographic Measurements

Transthoracic echocardiography was performed using a VEVO 2100 (Visual sonics) with a cardiac probe (MS-440D). Mice were anesthetized with isoflurane (1.5-1% in air), shaved with the use of depilatory cream, and placed on a dedicated heating plate in the supine position. During the procedure, heart rate (HR) and temperature (35-37°C) were monitored. Two-dimensional parasternal long-axis views at the level of the largest LV diameter were obtained for guided B-mode (mice subjected to myocardial infarction) and M-mode (sham-operated mice) measurements at the end of the diastole and systole. Endocardium contours were drawn from end-systolic and end-diastolic long-axis views; LV end-diastolic and-systolic volumes (Vd and

Vs respectively) were measured and percentage ejection fraction (EF) was then calculated ($EF = [(Vd - Vs) / Vd] \times 100$). The echocardiographic measurements were assessed in an external imaging platform by external experts, blinded to the genotype or the treatment of mice.

Immunohistochemistry

Fourteen days after MI, hearts were perfused with PBS. LV were mounted in Cryomatrix (Thermo Scientific) and dropped into frozen isopentane. Sections (7 μ m) were cut. For evaluation of apoptosis, heart sections and CM were stained with terminal deoxynucleotidyl transferase dUTP nick-end labeling (TUNEL) technology kit (Roche Diagnostics, Meylan, France) according to the manufacturer's instructions. Immunohistochemistry was performed using antibodies for IDO (clone 4B7, Merck), CD31 (clone MEC 7.46, Abcam) and cleaved caspase 3 (clone 9661, Cell Signaling). For Reactive Oxygen Species (ROS) visualization  in vivo, DHE (Dihydroethidium, Thermo Fisher Scientific) fluorescence staining was performed. Masson trichrome and Red Sirius stainings were completed to analyze infarct size and collagen content, respectively. Infarct size was expressed as the ratio of endocardial LV scar length to the total endocardial LV length. Collagen content and the number of capillaries were quantified in the border zone of the infarct scar on a Axioimager Carl Zeiss microscope. Collagen content was measured as the ratio of the total area stained by Red Sirius to the total area of the tissue section on the Image J software. Capillaries were stained with TRITC-conjugated Griffonia simplicifolia lectin (Sigma-Aldrich, Evry, France) and CM membranes with fluorescein isothiocyanate (FITC)-conjugated wheat germ agglutinin lectin (Sigma-Aldrich). Results were expressed as the ratio of capillaries number to CM. All quantifications were performed in a blinded manner without knowledge of mice genotype and treatment.

Cell isolation and culture

CM isolation protocol was performed as previously described²⁵. Briefly, heart was removed and perfused with buffer (130 mM NaCl, 5 mM KCl, 0.5 mM NaH₂PO₄, 10 mM HEPES, 10 mM glucose, 10 mM 2, 3-Butanedione Monoxime (BDM), 10 mM Taurine and 1.5 mM EDTA), then perfusion buffer (130 mM NaCl, 5 mM KCl, 0.5 mM NaH₂PO₄, 10 mM HEPES, 10 mM glucose, 10 mM BDM, 10 mM Taurine and 1 mM MgCl₂) after enzyme solution containing collagenase II (245 U/mg, Worthington Biochemical), collagenase IV (235 U/mg, Worthington Biochemical) and protease XIV (0.05 mg/mL, Sigma) for 80 ml/hour. CM cells were pelleted and suspended in calcium buffer containing CaCl₂ (0.125 μ M). Gradual calcium increments were done by adding, 5 μ l, 10 μ l, 30 μ l and 50 μ l of CaCl₂ (100 mM) with 4 minutes delay between each increase. For some conditions, CM were lysed for RNA extraction. For other conditions, CM (~10⁵ cells) were incubated in 24-well plate previously pre-coated with Laminin (50 μ g/ml, GibcoTM), in the presence or not of an AHR antagonist, CH-223191 (10 μ M), (Sigma-Aldrich) and/or in the presence of Kyn (10 μ M, Sigma) or vehicles. In other experiments, CM cells were incubated in the presence of either non-CM cells (CM/non-CM ratio= 1) or non-CM supernatants after 24 H of culture. ROS were visualized in red using CellRox Deep Red Reagent Kit (Life technologies).

For the study of CM contractility, cells were isolated as previously described²⁶. In some experiments, Kyn (100 μ M) was added in the medium for 90 min to test its effect on CM contractility. Cell shortening and calcium concentration were studied using CM stimulation at 0.5 Hz (20 V, 1 ms) at room temperature. Sarcomere length (SL) and fluorescence (405 and 480 nm) were simultaneously recorded using Ion Wizard/IonOptix 6.6 software (IonOptix system, Hilton, USA) connected to an inverted fluorescence microscope.

SMC were prepared from mouse thoracic aorta as previously described²⁷. SMC were stimulated with lipopolysaccharide (LPS) (1 µg/ml) and IFN-γ (100 U/ml) for 24 hours. Cells were then lysed for RNA extraction.

Flow Cytometry and cell sorting

Hearts were collected and the LV was isolated, minced with fine scissors, and gently passed through the Bel-Art Scienceware 12-Well Tissue Disaggregator (Fisher Scientific). Cells were collected, filtered through 40-µm nylon mesh, and washed with PBS. Red blood cells were removed by incubation in hemolysis buffer (Sigma Life Science). Cells were stained for flow cytometry at 4°C. Total cardiac cells were gated on Alexa Fluor 700 anti-mouse CD45 (30-F11, Biolegend), and the following antibodies were used: Brilliant Violet (BV) 605 anti-mouse/human CD11b (M1/70, Biolegend), phycoerythrin (PE)-conjugated anti-Hu/Mo CD45R (B220) (RA3-6B2, eBioscience), PE-Cy7 Hamster Anti-Mouse CD3e (145-2C11, BD Pharmingen, BD Biosciences), BV 650 Rat Anti-Mouse CD4 (RM 4-4, BD Opti Build, BD Biosciences), PerCP-Cy5,5 Rat Anti-Mouse CD8a (53-6.7, BD Pharmingen, BD Biosciences), allophycocyanin-conjugated anti-F4/80 (MCA497, AbD Serotec, Bio-Rad), fluorescein isothiocyanate (FITC) Rat Anti-Mouse Ly-6C (AL-21, BD Pharmingen, BD Biosciences), BUV 395 Rat Anti-Mouse Ly6G (1A8, BD Horizon, BD Biosciences). The total number of cells was then normalized to heart weight. Events were acquired on an LSR II flow cytometer (BD Biosciences) and results were analyzed on FlowJo software. In other experiments, non-CM cells were stained with Rat Anti-Mouse CD16/CD32 (2.4G2, BD PharmingenTM) antibody in order to block Fc receptors. Then cells were stained with PE-conjugated Rat anti-CD31 (MEC 13.3, BD Biosciences) and FITC Rat anti-CD45 (30-F11, BD Biosciences). EC (CD45- CD31+) and leukocytes (CD45+CD31-) in non-CM fraction were isolated by using FACS Aria II (BD Biosciences).

Quantitative Real time PCR

Cells were lysed in detergent buffer RLT (1:100 β -Mercaptoethanol) and then subjected to RNA extraction and reverse transcription (Qiagen). Quantitative real-time PCR was performed on an ABI PRISM 7700 (Applied Biosystems) in triplicates. Cycle threshold for Gapdh (primers: Gapdh-R, 5'-CGTCCCGTAGACAAAATGGTGAA-3'; Gapdh-L, 5'-GCCGTGAGTGGAGTCATACTGGAACA-3') was used to normalize gene expression. Primers for *Ido-1* are: *Ido-1*-R, 5'-ATATATGCGGAGAACGTGGAAAAAC -3', *Ido-1*-L 5'-CAATCAAAGCAATCCCCACTGTATC-3'. PCR conditions were 10 min at 95°C; 35 cycles of 95°C for 15 s, 60°C for 20 s, and 72°C for 20 s; and a final extension at 72°C for 20s.

HPLC Quantifications

Some plasma, heart, supernatant and cell samples were subjected to HPLC quantifications, as previously described⁴. The plasma samples and standards containing equal volume of 3-nitro- L-tyrosine (1 μ M) were deproteinized by 25 μ l of 2 M trichloroacetic acid. The proteins were pelleted by centrifugation at 10,000 rpm for 6 minutes. The supernatants were injected in autosampler (Waters) for detection of Trp by its autofluorescence at an excitation wavelength of 286 nm and emission wavelength of 366 nm. Kyn was detected by UV absorption at 360 nm. The measurements of Trp, Kyn, AA, Kna, 3-OHKyn, 3HAA and Quina on heart and Kyn and Trp on cell homogenates were performed as previously described²⁸. IDO activity was assessed as the Kyn/Trp ratio. Heart and cell lysis were achieved by mechanical disruption in an ice-cold modified Tyrode buffer (3013m Osm/l, pH 7.40) using a Teflon-glass homogenizer (5 min, 2200 rpm at 4°C), followed by an -SH-activated toxin treatment as previously described²⁹.

Statistical analysis

Groups of animals were pre-defined according to genotype and active treatment versus vehicle, and were matched for age and sex. One-way ANOVA was used to compare each measure when there were ≥ 3 independent groups. Two-way ANOVA was used to evaluate the effect of two categorical variables. Comparisons between groups were then performed using the Tukey's multiple comparisons when the ANOVA test was statistically significant. The Mann-Whitney test was used to compare 2 groups. Values are expressed as means \pm s.e.m. Values were considered significant at $P < 0.05$. All statistical tests were performed using GraphPad PRISM software version 8.3.1.

Results



Up-regulation of IDO activity after MI alters cardiac function and remodeling

To investigate the time-dependent regulation of IDO activity, we assessed the Kyn/Trp ratio in WT mice challenged with either sham surgery or MI for 1, 3, 5, 7 or 14 days. As shown in

Figure 1A, IDO activity is markedly induced in the heart as early as day 1 after MI compared to sham-operated WT mice. The Kyn/Trp ratio is also increased in plasma (**Figure 1B**) at day 1 after MI, and peaks at day 7 after the onset of ischemia. We next evaluated the role of IDO on cardiac function in WT and IDO-deficient (*Ido-1^{-/-}*) mice either sham-operated or subjected to MI. Remarkably, we found that loss of function of IDO attenuated cardiac dysfunction after MI, as revealed by a significant improvement of LV EF and a decrease in Vd and Vs (**Figure 1C**).

We next assessed whether pharmacological inhibition of IDO activity by L-1MT could recapitulate the beneficial impact of IDO deficiency. IDO activity inhibition by L-1MT, as revealed by a decrease in plasma Kyn/Trp ratio (**Figure 1D**), improved cardiac function in

comparison with control mice subjected to MI (**Figure 1E**). Attenuation of cardiac dysfunction in absence of IDO activity was associated with a decrease in adverse LV remodeling. We observed a smaller infarct size as well as less interstitial fibrosis in *Ido-1*^{-/-} and L-1MT-treated animals in comparison with WT and untreated mice, respectively, 14 days after MI (**Figure 2A-B**). Moreover, IDO deficiency, but not L-1MT treatment, improved capillary numbers as compared with WT mice (**Figure 2C**). This discrepancy could be accounted by the marked decrease in Kyn/Trp ratio in IDO deficient mice compared to L-1MT treated animals. Interestingly, cardiac lactate levels (**Supplemental Figure I**) as well as apoptotic cell number, as assessed by TUNEL staining, were also decreased in *Ido-1*^{-/-} and L-1MT-treated mice compared to WT animals (**Figure 2D**).

Ido-1 deficiency could decrease infarct size and attenuate cardiac dysfunction through modulation of inflammation. Accordingly, since IDO is known to be expressed in inflammatory cells such as macrophages¹⁸, we first examined whether the number of infiltrating inflammatory cells in the infarcted heart was modulated by IDO deficiency. Using flow cytometry, we evaluated the number of Ly-6C^{high} and Ly-6C^{low} monocytes, neutrophils and T lymphocytes within the myocardium at day 0, 3 or 7 after coronary ligation. As shown in the **Supplemental Figure II**, no significant differences in the number of cardiac T CD4⁺ cells, monocytes and neutrophils were observed between WT and *Ido-1*^{-/-} mice. Similarly, cardiac Tregs number was comparable in WT and *Ido-1*^{-/-} mice (**Supplemental Figure II**). Next, we assessed the role of BM-derived inflammatory cells expressing IDO. For this purpose, we generated WT and *Ido-1*^{-/-} chimeras lethally irradiated and transplanted with BM-derived cells isolated from WT or *Ido-1*^{-/-} mice. After induction of MI, no differences in cardiac function, infarct size and capillary density were observed between WT mice transplanted with BM from either WT or *Ido-1*^{-/-} cells (**Figure**

3A-B). In contrast, cardiac function was improved in *Ido-1*^{-/-} mice transplanted with BM isolated from either WT or *Ido-1*^{-/-} cells, compared to WT chimeras (**Figure 3A**). Consistently, infarct size and capillary number were also improved (**Figure 3B**). Altogether, these results suggest that inflammatory cells expressing IDO do not participate to the regulation of cardiac function and support a crucial role for IDO expressed in non BM-derived cells.

We then aimed to determine whether CM expressing IDO could affect cardiac homeostasis. Loss of function of IDO improved ex vivo contractility of CM isolated after acute MI, as assessed by high contraction and relaxation velocities (**Supplemental Figure III**). We therefore hypothesized that IDO expressed in CM was a major regulator of cardiac remodeling and function. CM deficiency was achieved by crossbreeding α -MHC-MerCre animals in which the CM-specific Myh6 promoter drives expression of a 4-OH-tamoxifen-inducible Cre recombinase fusion protein with *Ido-1*^{flox/flox} mice (*Ido-1*^{flox/flox} α MHC-Cre or CM IDO KO). After tamoxifen treatment, IDO expression was markedly decreased in CM (**Figure 3C**). However, as shown in **Figure 3D** and **E**, cardiac function and remodeling were unaffected in CM IDO KO when compared to their wild-type littermates (CM IDO), suggesting that CM are not the major source of IDO in heart and that non-CM IDO-expressing cells govern IDO-related effects on the cardiac tissue. We then postulated that vascular cells such as SMC and EC, which are known to express IDO^{19, 30}, were involved in IDO-related effects on cardiac tissue. Consistently, IDO expression was observed in the vessels of infarcted heart (**Supplemental Figure III**). To test the role of IDO expressed in SMC, we developed mice with a specific deletion of IDO in this cell type (*Ido-1*^{flox/flox} SMC22-Cre or SMC IDO KO) and challenged them with MI. Although a marked reduction in IDO expression was observed in SMC, cardiac function and healing were unchanged in SMC IDO KO mice when compared to their wild-type littermates (**Supplemental**

Figure III), indicating that IDO expressed in SMC was not involved in the regulation cardiac function in our experimental conditions.

IDO expressed by EC alters cardiac function and remodeling

We next speculated that IDO expressed in EC could participate to the cardiac phenotype.

Interestingly, IDO activity (Kyn/Trp) was higher in isolated cardiac EC compared to CM or leukocytes, after MI (**Figure 4A**). Consistently, *Ido-1 mRNA* was 13-fold higher in isolated cardiac EC compared to CM (**Figure 4B**), unravelling the importance of IDO expressed in EC.

We then analyzed the role of EC expressing IDO using mice with specific conditional deletion of IDO in EC (*Ido-1^{flox/flox} VECad-CreERT2⁺* or EC IDO KO). We found that *Ido-1 mRNA* expression was dampened in EC isolated from heart of EC IDO KO animals (**Figure 4B**).

Moreover, Kyn/Trp ratio was significantly reduced in LV heart extracts of EC IDO KO compared to control animals, after MI (**Figure 4C**). Interestingly, cardiac function of EC IDO KO mice subjected to MI was markedly improved compared to their WT controls (EC IDO) (**Figure 4D**). This was associated with a reduction in infarct size, interstitial fibrosis, and apoptosis (**Figure 4E-G**). Altogether, these results indicated that cardiac function recovery was dependent on IDO expression in EC but not in SMC, inflammatory cells or CM.

Kyn alters cardiac function and remodeling

Then, we analyzed the molecular and cellular mechanisms associated with IDO detrimental effects on cardiac tissue. We measured the IDO activity-related metabolites in the cardiac tissue (**Supplemental Figure IV**). Kyn levels were significantly increased in the heart and plasma as early as day 1 after MI (**Supplemental Figure IV**), compared to sham-operated WT mice.

Concentrations of Kyn-derived metabolites including AA, 3-HAA, Kna and Quina, were 100 to 1000-fold lower when compared to that of Kyn. Furthermore, their cardiac levels did not

significantly change after MI or were even decreased as for 3-OHKyn (**Supplemental Figure IV**), suggesting a minor role for those metabolites in acute MI.

We thus hypothesized that IDO exerted its deleterious role on cardiac outcome through Kyn production. *Ido-1*^{-/-} mice were supplemented with Kyn and subjected to MI. As shown in (**Figure 5A-D**), Kyn supplementation was associated with an aggravation of cardiac function as well as a deleterious cardiac remodeling as revealed by lower capillary number and increased infarct size and interstitial fibrosis. As Kyn pathway is instrumental in the regulation of apoptosis^{6, 22}, we hypothesized that Kyn could negatively affect cardiac remodeling through induction of CM apoptosis. Consistently, *in vivo* Kyn supplementation in *Ido-1*^{-/-} mice fostered cell apoptosis in infarcted heart (**Figure 5E** and **Supplemental Figure V**) as well as CM apoptosis *in vitro* (**Supplemental Figure V**). In addition, in CM Kyn up-regulated the production of ROS (**Figure 5F**), potent activators of apoptosis³¹. Kyn is known to act as an endogenous agonist of the AHR³². We then determined whether the blockade of AHR activity could abolish the Kyn-induced pro-apoptotic effect. CM were incubated with the AHR inhibitor (CH-223191), with or without Kyn. As shown in the **Supplemental Figure V**, incubation of CM with Kyn in the presence of an AHR inhibitor abrogated the Kyn-induced pro-apoptotic effect, as well as Kyn-induced ROS production, suggesting that AHR mediated the effect of Kyn on CM apoptosis. Importantly, the *in vivo* pro-apoptotic effect of Kyn was abolished after AHR antagonist administration to IDO KO mice, as compared to mice treated with AHR antagonist vehicle (**Figure 5G**).

As a decrease in apoptosis was observed in EC IDO KO hearts after MI (Fig. 4E), we speculated that Kyn produced by EC might affect CM apoptosis and contractility *via* paracrine effects. Consistently, EC-specific IDO KO led to a marked decrease in Kyn in the non-CM cells

(**Supplemental Figure V**) and in non-CM supernatants (**Figure 6A**), highlighting the importance of EC in cardiac Kyn production. Moreover, CM apoptosis was increased in the presence of non-CM cells (**Supplemental Figure V**) or supernatants of cultured non-CM cells (**Figure 6B**) isolated from infarcted heart as compared to sham-operated heart. CM apoptosis was reduced in the presence of supernatant of non-CM cells isolated from EC IDO KO mice (**Figure 6B**). In addition, ROS production was reduced in the peri-infarcted area of EC-specific IDO KO when compared to their WT littermates (**Figure 6C**). Interestingly, the specific deletion of IDO in EC improved ex vivo contractility of CM cells isolated from EC IDOKO mice 14 days post MI (**Figure 6D**). Moreover, as shown in the **Supplemental Figure VI**, *in vitro* Kyn supplementation reduced relaxation velocity of IDO KO CM cells. These results suggest that the increase in Kyn production within EC exerted deleterious effects on CM, which may contribute to worse cardiac outcome after MI.

Discussion

In the present study, we show for the first time that IDO deficiency attenuates cardiac dysfunction after MI and that Kyn, one the major IDO-related metabolites, conveys the deleterious effects of IDO on cardiac remodeling. Previous studies have already underlined the damaging impact of IDO-dependent pathways on cardiovascular system. IDO has been shown to promote the development of atherosclerosis¹¹, through inhibition of a major immune-regulatory and athero-protective cytokine, IL-10³³. The induction of IDO by dietary microbial oxazoles also reduced IL-10 production in intestinal epithelial cells²¹. On the same note, clinical studies showed that circulating Kyn, a major IDO-related metabolites, was associated with cardiovascular risk factors^{34, 35} and with worse cardiovascular outcome¹²⁻¹⁴.

IDO is induced in the context of inflammatory diseases¹⁸. MI is associated with an intense inflammatory reaction through the production of cytokines, such as TNF- α , and IL-6, that are known to foster IDO expression and activity^{16,36}. TNF- α , and IL-6 upregulation in the acute post-infarction period is under the control of hypoxia and ROS. The increased cardiac IDO activity, within the first day after MI, may therefore depend on the induction of such ischemia-associated inflammatory cytokines. IDO is known as an immunosuppressive factor through breakdown of Trp and generation of some metabolites, which induced inactivation or apoptosis of effector T cells¹⁸. However, in our study, we did not find any significant differences in the infiltration of T cells or Tregs within the infarcted hearts of IDO KO mice as compared to controls, suggesting that such mechanisms were not involved in the deleterious IDO-related effects on cardiac remodeling. In line with these results, the lack of IDO in BM-derived inflammatory cells did not affect post-MI cardiac outcome.

Vascular cells such as SMC and EC have been shown to express IDO^{19,30}. We thus postulated that IDO localized in the vascular compartment could impact cardiac remodeling and function. Mice with endothelial-, but not SMC-specific IDO deletion, subjected to coronary ligation exhibited less interstitial fibrosis, and CM apoptosis, leading to greater preservation of LV systolic function as compared to control mice, thereby revealing the importance of IDO expression in cardiac EC. Total and EC-specific deletion of IDO were associated with a decrease in apoptosis in ischemic heart after MI. This was substantiated by *in vitro* studies showing that IDO deletion in EC protected against CM apoptosis, and that Kyn was responsible for these pro-apoptotic effects, most likely through ROS production. *In vivo*, Kyn reversed the protective effects of IDO deficiency, suggesting that the increase in Kyn *via* upregulation of IDO in EC was involved in the detrimental effects on cardiac remodeling after MI. Moreover, CM

isolated from EC IDO KO mice displayed better contractility highlighting the preeminent role of the crosstalk between EC and CM in the regulation of cardiac function.

Cardiac cells communicate with each other through direct cell interactions and paracrine pathways, to shape signaling mechanisms in the injured cardiac tissue. Particularly, CM and EC are two of the most abundant cardiac cell types and they also play central roles in cardiac remodeling. Recent evidence underlined the importance of EC, not only as the most abundant non-myocyte cell type in the heart, but also as key players in post-infarction remodeling³⁷. In our study, despite the fact that IDO expression and activity were detected in CM, IDO expression in these cells did not affect cardiac outcome after MI. Interestingly, IDO expression or activity, as assessed by Kyn/Trp ratio, in cardiac EC was much higher than that in CM, suggesting that IDO in EC, but not in CM, is a major reservoir of Kyn in the cardiac tissue. Nevertheless, EC and CM communicate with each other and this could account for the effect of EC-IDO derived metabolites on CM apoptosis and contractility, although the mechanisms of this crosstalk are not completely elucidated. The importance of EC-derived IDO was further highlighted by the fact that the non-CM fraction obtained from mice with the specific IDO deletion in EC after MI markedly decreased Kyn levels and protected CM against apoptosis. Hence, EC-derived IDO exerted pro-apoptotic effects on CM. Our results are consistent with previous observations showing that Kyn or Kyn-derived metabolites have detrimental effects on apoptosis^{6, 19}. Kyn has been identified as an endogenous ligand for AHR³², and Kyn/AHR interaction exerted deleterious role during cerebral ischemia³⁸. On the same note, EC-specific AHR knockout mice exhibited hypotension and blunted response to angiotensin II³⁹. Moreover, AHR may have deleterious effects in myocardial ischemia⁴⁰. In our experimental conditions, we showed that the apoptotic effects on CM, as well as ROS induction by Kyn, were dependent on AHR since its

inactivation prevented the Kyn-mediated effects. The *in vivo* pro-apoptotic effects of Kyn were also blunted after administration of the AHR antagonist. Altogether, our data underscore the paracrine effects of EC-producing Kyn on CM apoptosis.

In conclusion, our findings show that IDO inhibitor, as well as the total and the specific endothelial deletion of IDO, protect against the deleterious cardiac effects of MI-induced ischemia. In contrast, Kyn supplementation, a major IDO-related metabolite, abolishes the protective effects of IDO deficiency in this setting. Inhibition of IDO activity might represent a novel potential therapeutic strategy to mitigate ischemic cardiac injury.

Acknowledgments

We are grateful to the imaging platform for small animals of Paris Descartes University (Carmen Marchiol, Franck Lager and Gilles Renault) for echocardiographic analysis and Camille Brunaud for performing cell sorting experiments.

Sources of Funding

This work was supported by Institut National de la santé et de la recherche médicale (INSERM) and Agence Nationale de la recherche (ANR to S.T.) and FRM (*Fondation pour la Recherche Médicale*), DEQ20161136699, to AT, ST and HAO. N-J.M. was the recipient of fellowships from the FRM (FDT201904008169) and Lebanese Association for Scientific Research (LASeR) for thesis and GRRC (*Groupe de Réflexion sur la Recherche Cardiovasculaire*) travel grant. M.C. was the recipient of fellowships from ANR and FRM.

Authors

Nada Joe Melhem, PhD¹; Mouna Chajadine, MS¹; Ingrid Gomez, PhD¹;
 Kiave-Yune Howangyin, PhD¹; Marion Bouvet, PhD¹; Camille Knosp, PhD¹; Yanyi Sun, MD¹;
 Marie Rouanet, PhD¹; Ludivine Laurans, PhD¹; Olivier Cazorla, PhD²; Mathilde Lemitre, BS¹;
 José Vilar, PhD¹; Ziad Mallat, MD, PhD^{1,3}; Alain Tedgui, PhD¹; Hafid Ait-Oufella, MD, PhD¹;
 Jean-Sébastien Hulot, MD, PhD¹; Jacques Callebort, Pharm. D, PhD⁴;
 Jean-Marie Launay, MD, PhD⁴; Jeremy Fauconnier, PhD²; Jean-Sébastien Silvestre, PhD¹;
 Soraya Taleb, PhD¹

¹Université de Paris, PARCC, Inserm, F-75015 Paris, France; ²PHYMEDEXP, Inserm, CNRS, Université de Montpellier, CHRU Montpellier, Montpellier, France; ³Division of Cardiovascular Medicine, University of Cambridge, Addenbrooke's Hospital, Cambridge, CB2 2QQ, UK; ⁴Service de Biochimie, Assistance Publique Hôpitaux de Paris, and INSERM UMR942, Hôpital Lariboisière, Paris, France

Disclosures

None.

Supplemental Material

Supplemental Figures I - VI

References

1. Silvestre JS, Smadja DM, Levy BI. Postischemic revascularization: From cellular and molecular mechanisms to clinical applications. *Physiol Rev.* 2013;93:1743-1802

2. Romani L, Zelante T, De Luca A, Fallarino F, Puccetti P. IL-17 and therapeutic kynurenines in pathogenic inflammation to fungi. *J Immunol*. 2008;180:5157-5162
3. Schwarcz R, Kohler C. Differential vulnerability of central neurons of the rat to quinolinic acid. *Neuroscience letters*. 1983;38:85-90
4. Laurans L, Venteclef N, Haddad Y, Chajadine M, Alzaid F, Metghalchi S, Sovran B, Denis RGP, Dairou J, Cardellini M, et al. Genetic deficiency of indoleamine 2,3-dioxygenase promotes gut microbiota-mediated metabolic health. *Nat Med*. 2018;24:1113-1120
5. Wang Q, Ding Y, Song P, Zhu H, Okon I, Ding YN, Chen HZ, Liu DP, Zou MH. Tryptophan-derived 3-hydroxyanthranilic acid contributes to angiotensin II-induced abdominal aortic aneurysm formation in mice in vivo. *Circulation*. 2017;136:2271-2283
6. Metghalchi S, Vandestienne M, Haddad Y, Esposito B, Dairou J, Tedgui A, Mallat Z, Potteaux S, Taleb S. Indoleamine 2,3-dioxygenase knockout limits angiotensin II-induced aneurysm in low density lipoprotein receptor-deficient mice fed with high fat diet. *PLoS One*. 2018;13:e0193737
7. Nakajima K, Yamashita T, Kita T, Takeda M, Sasaki N, Kasahara K, Shinohara M, Rikitake Y, Ishida T, Yokoyama M, et al. Orally administered eicosapentaenoic acid induces rapid regression of atherosclerosis via modulating the phenotype of dendritic cells in LDL receptor-deficient mice. *Arterioscler Thromb Vasc Biol*. 2011;31:1963-1972
8. Polyzos KA, Ovchinnikova O, Berg M, Baumgartner R, Agardh H, Pirault J, Gistera A, Assinger A, Laguna-Fernandez A, Back M, et al. Inhibition of indoleamine 2,3-dioxygenase promotes vascular inflammation and increases atherosclerosis in apoE^{-/-} mice. *Cardiovasc Res*. 2015;106:295-302
9. Zhang L, Ovchinnikova O, Jonsson A, Lundberg AM, Berg M, Hansson GK, Ketelhuth DF. The tryptophan metabolite 3-hydroxyanthranilic acid lowers plasma lipids and decreases atherosclerosis in hypercholesterolaemic mice. *Eur Heart J*. 2012;33:2025-2034
10. Cole JE, Astola N, Cribbs AP, Goddard ME, Park I, Green P, Davies AH, Williams RO, Feldmann M, Monaco C. Indoleamine 2,3-dioxygenase-1 is protective in atherosclerosis and its metabolites provide new opportunities for drug development. *Proc Natl Acad Sci U S A*. 2015;112:13033-13038
11. Metghalchi S, Ponnuswamy P, Simon T, Haddad Y, Laurans L, Clement M, Dalloz M, Romain M, Esposito B, Koropoulis V, et al. Indoleamine 2,3-dioxygenase fine-tunes immune homeostasis in atherosclerosis and colitis through repression of interleukin-10 production. *Cell metabolism*. 2015;22:460-471
12. Pedersen ER, Midttun O, Ueland PM, Schartum-Hansen H, Seifert R, Igland J, Nordrehaug JE, Ebbing M, Svingen G, Bleie O, et al. Systemic markers of interferon-gamma-mediated immune activation and long-term prognosis in patients with stable coronary artery disease. *Arterioscler Thromb Vasc Biol*. 2011;31:698-704
13. Pedersen ER, Tuseh N, Eussen SJ, Ueland PM, Strand E, Svingen GF, Midttun O, Meyer K, Mellgren G, Ulvik A, et al. Associations of plasma kynurenines with risk of acute myocardial infarction in patients with stable angina pectoris. *Arterioscler Thromb Vasc Biol*. 2015;35:455-462
14. Eussen SJ, Ueland PM, Vollset SE, Nygard O, Midttun O, Sulo G, Ulvik A, Meyer K, Pedersen ER, Tell GS. Kynurenines as predictors of acute coronary events in the Hordaland Health Study. *Int J Cardiol*. 2015;189:18-24

15. Pawlak K, Brzosko S, Mysliwiec M, Pawlak D. Kynurenine, quinolinic acid--the new factors linked to carotid atherosclerosis in patients with end-stage renal disease. *Atherosclerosis*. 2009;204:561-566
16. O'Connor JC, Andre C, Wang Y, Lawson MA, Szegedi SS, Lestage J, Castanon N, Kelley KW, Dantzer R. Interferon-gamma and tumor necrosis factor-alpha mediate the upregulation of indoleamine 2,3-dioxygenase and the induction of depressive-like behavior in mice in response to bacillus calmette-guerin. *The Journal of neuroscience : the official journal of the Society for Neuroscience*. 2009;29:4200-4209
17. Chon SY, Hassanain HH, Gupta SL. Cooperative role of interferon regulatory factor 1 and p91 (stat1) response elements in interferon-gamma-inducible expression of human indoleamine 2,3-dioxygenase gene. *J Biol Chem*. 1996;271:17247-17252
18. Mellor AL, Munn DH.IDO expression by dendritic cells: Tolerance and tryptophan catabolism. *Nature reviews. Immunology*. 2004;4:762-774
19. Wang Y, Liu H, McKenzie G, Witting PK, Stasch JP, Hahn M, Changsirivathanathamrong D, Wu BJ, Ball HJ, Thomas SR, et al. Kynurenine is an endothelium-derived relaxing factor produced during inflammation. *Nat Med*. 2010;16:279-285
20. Mohib K, Wang S, Guan Q, Mellor AL, Sun H, Du C, Jevnikar AM. Indoleamine 2,3-dioxygenase expression promotes renal ischemia-reperfusion injury. *Am J Physiol Renal Physiol*. 2008;295:F226-234
21. Iyer SS, Gensollen T, Gandhi A, Oh SF, Neves JF, Collin F, Lavin R, Serra C, Glickman J, de Silva PSA, et al. Dietary and microbial oxazoles induce intestinal inflammation by modulating aryl hydrocarbon receptor responses. *Cell*. 2018;173:1123-1134 e1111
22. Wang Q, Zhang M, Ding Y, Wang Q, Zhang W, Song P, Zou MH. Activation of nad(p)h oxidase by tryptophan-derived 3-hydroxykynurenine accelerates endothelial apoptosis and dysfunction in vivo. *Circ Res*. 2014;114:480-492
23. Blenck CL, Harvey PA, Reckelhoff JF, Leinwand LA. The importance of biological sex and estrogen in rodent models of cardiovascular health and disease. *Circ Res*. 2016;118:1294-1312
24. Zouggar Y, Ait-Oufella H, Bonnin P, Simon T, Sage AP, Guerin C, Vilar J, Caligiuri G, Tsiantoulas D, Laurans L, et al. B lymphocytes trigger monocyte mobilization and impair heart function after acute myocardial infarction. *Nat Med*. 2013;19:1273-1280
25. Ackers-Johnson M, Li PY, Holmes AP, O'Brien SM, Pavlovic D, Foo RS. A simplified, langendorff-free method for concomitant isolation of viable cardiac myocytes and nonmyocytes from the adult mouse heart. *Circ Res*. 2016;119:909-920
26. Fauconnier J, Lanner JT, Sultan A, Zhang SJ, Katz A, Bruton JD, Westerblad H. Insulin potentiates trpc3-mediated cation currents in normal but not in insulin-resistant mouse cardiomyocytes. *Cardiovasc Res*. 2007;73:376-385
27. Cherepanova OA, Gomez D, Shankman LS, Swiatlowska P, Williams J, Sarmiento OF, Alencar GF, Hess DL, Bevard MH, Greene ES, et al. Activation of the pluripotency factor oct4 in smooth muscle cells is atheroprotective. *Nat Med*. 2016;22:657-665
28. Laugeray A, Launay JM, Callebort J, Surget A, Belzung C, Barone PR. Evidence for a key role of the peripheral kynurenine pathway in the modulation of anxiety- and depression-like behaviours in mice: Focus on individual differences. *Pharmacol Biochem Behav*. 2011;98:161-168

29. Launay JM, Geoffroy C, Costa JL, Alouf JE. Purified -sh-activated toxins (streptolysin o, alveolysin): New tools for determination of platelet enzyme activities. *Thrombosis research*. 1984;33:189-196
30. Cuffy MC, Silverio AM, Qin L, Wang Y, Eid R, Brandacher G, Lakkis FG, Fuchs D, Pober JS, Tellides G. Induction of indoleamine 2,3-dioxygenase in vascular smooth muscle cells by interferon-gamma contributes to medial immunoprivilege. *J Immunol*. 2007;179:5246-5254
31. Redza-Dutordoir M, Averill-Bates DA. Activation of apoptosis signalling pathways by reactive oxygen species. *Biochimica et biophysica acta*. 2016;1863:2977-2992
32. Opitz CA, Litzenburger UM, Sahm F, Ott M, Tritschler I, Trump S, Schumacher T, Jestaedt L, Schrenk D, Weller M, et al. An endogenous tumour-promoting ligand of the human aryl hydrocarbon receptor. *Nature*. 2011;478:197-203
33. Mallat Z, Besnard S, Duriez M, Deleuze V, Emmanuel F, Bureau MF, Soubrier F, Esposito B, Duez H, Fievet C, et al. Protective role of interleukin-10 in atherosclerosis. *Circ Res*. 1999;85:e17-24
34. Pertovaara M, Raitala A, Juonala M, Lehtimäki T, Huhtala H, Oja SS, Jokinen E, Viikari JS, Raitakari OT, Hurme M. Indoleamine 2,3-dioxygenase enzyme activity correlates with risk factors for atherosclerosis: The cardiovascular risk in young finns study. *Clinical and experimental immunology*. 2007;148:106-111
35. Niinisalo P, Raitala A, Pertovaara M, Oja SS, Lehtimäki T, Kahonen M, Reunanen A, Jula A, Moilanen L, Kesaniemi YA, et al. Indoleamine 2,3-dioxygenase activity associates with cardiovascular risk factors: The health 2000 study. *Scandinavian journal of clinical and laboratory investigation*. 2008;68:767-770
36. Nian M, Lee P, Khaper N, Liu P. Inflammatory cytokines and postmyocardial infarction remodeling. *Circ Res*. 2004;94:1543-1553
37. Pinto AR, Ilinykh A, Ivey MJ, Kuwabara JT, D'Antoni ML, Debuque R, Chandran A, Wang L, Arora K, Rosenthal NA, et al. Revisiting cardiac cellular composition. *Circ Res*. 2016;118:400-409
38. Cuartero MI, Ballesteros I, de la Parra J, Harkin AL, Abautret-Daly A, Sherwin E, Fernandez-Salguero P, Corbi AL, Lizasoain I, Moro MA. L-kynurenine/aryl hydrocarbon receptor pathway mediates brain damage after experimental stroke. *Circulation*. 2014;130:2040-2051
39. Agbor LN, Elased KM, Walker MK. Endothelial cell-specific aryl hydrocarbon receptor knockout mice exhibit hypotension mediated, in part, by an attenuated angiotensin ii responsiveness. *Biochem Pharmacol*. 2011;82:514-523
40. Wang B, Xu A. Aryl hydrocarbon receptor pathway participates in myocardial ischemia reperfusion injury by regulating mitochondrial apoptosis. *Med Hypotheses*. 2019;123:2-5

Figure Legends

Figure 1. IDO deficiency or inhibition limits cardiac dysfunction after MI

A-B, Time-dependent monitoring of cardiac (**A**) and plasma (**B**) IDO activity (Kyn/Trp) in wild-type (WT) mice challenged with MI compared to sham-operated mice at day 1, 3, 5, 7 or 14 after surgery (n=3-5 mice per time point). **C**, Quantitative evaluation of left ventricle (LV) ejection fraction (left), LV systolic (middle) and diastolic (right) volumes in WT and *Ido-1^{-/-}* mice either sham-operated (n=5 per group) or challenged with MI (n=10 per group). Two-way ANOVA was used followed by Tukey's multiple comparisons test. **D**, Circulating IDO activity (Kyn/Trp) measured before MI, in 1-Methyl-L-Tryptophan (L-1MT)-treated WT mice (n=5) compared to non-treated WT mice (n=8). **E**, Quantitative evaluation of LV ejection fraction (left), LV systolic (middle) and diastolic (right) volumes in L-1MT-treated WT mice compared to non-treated WT mice challenged with MI (n=14 per group). Cardiac function was evaluated at day 14 after MI. Mann Whitney test was used to compare WT vs L-1MT-treated groups. Individual data are presented as aligned dot plots, with the mean and s.e.m. * $P < 0.05$, ** $P < 0.01$, *** $P < 0.001$.

Figure 2. IDO deficiency or inhibition improves cardiac healing after MI

A, Quantification and representative photomicrographs of infarct size in wild-type (WT) (n=29), *Ido-1^{-/-}* (n=11) and 1-Methyl-L-Tryptophan (L-1MT)-treated (n=13) mice challenged with myocardial infarction (MI). One-way ANOVA was used followed by Tukey's multiple comparisons test. **B-C**, Quantitative evaluation of interstitial fibrosis (**B**) and capillary density (**C**) in WT and *Ido-1^{-/-}* mice either sham-operated (n=10 for WT and n=5 for IDOKO mice) or challenged with MI as well as in L-1MT-treated WT mice after MI. Two-way ANOVA was used

followed by Tukey's multiple comparisons test. **D**, TUNEL (terminal deoxynucleotidyl transferase-mediated dUTP nick end-labeling) quantification and representative images (right) in the peri-infarcted area of the LV of *Ido-1*^{-/-} mice and L-1MT-treated WT mice compared to their control littermates at day 2 post-MI. Arrows point to apoptotic nuclei. Representative images are presented. Cardiac remodeling was evaluated at day 14 after MI. One-way ANOVA was used followed by Tukey's multiple comparisons test. Individual data are presented as aligned dot plots, with the mean and s.e.m. * $P < 0.05$, ** $P < 0.01$, *** $P < 0.001$.

Figure 3. IDO specific deficiency in bone marrow-derived cells or cardiomyocytes does not control cardiac function and remodeling after MI

A-B, Quantitative analysis of left ventricle (LV) ejection fraction, LV systolic and diastolic volumes (**A**), infarct size and capillary density (**B**) in wild-type (WT) and *Ido-1*^{-/-} lethally irradiated and transplanted with bone marrow (BM)-derived cells isolated from WT or *Ido-1*^{-/-} mice and then challenged with myocardial infarction (MI) (n=6-14 per group). One-way ANOVA was used followed by Tukey's multiple comparisons test. **C**, *Ido-1* mRNA in cardiomyocytes isolated from the left ventricle (LV) of IDO deficient mice (CM IDOKO) (n=4) compared to their control littermates (CM IDO) (n=4). **D-E**, Quantitative evaluation of left ventricle (LV) ejection fraction, LV systolic and diastolic volumes (**D**), infarct size, interstitial fibrosis and capillary density (**E**) in cardiomyocyte IDO deficient mice (CM IDOKO) (n=12) compared to their control littermates (CM IDO) (n=13), challenged with MI. Representative images are presented. Cardiac function and remodeling were evaluated at day 14 after MI. Mann Whitney test was used to compare CM IDO vs CM IDOKO groups. Individual data are presented as aligned dot plots, with the mean and s.e.m. * $P < 0.05$, ** $P < 0.01$, *** $P < 0.001$.

Figure 4. IDO specific deficiency in endothelial cell limits cardiac dysfunction and deleterious remodeling after MI

A, IDO activity (Kyn/Trp) in fluorescence-activated cell-sorted cardiac endothelial cells (EC) (CD31+CD45-), leukocytes (CD31-CD45+) and cardiomyocytes (CM) isolated from the left ventricle (LV) of WT mice (n=9), 1 day after myocardial infarction (MI) (n=3/per group). Each point represents Kyn/Trp ratio of pooled cells isolated from 3 WT mice challenged with MI. **B**, *Ido-1* mRNA expression in pooled CM isolated from the left ventricle (LV) of WT mice (n=9) and in fluorescence-activated cell-sorted cardiac EC isolated from non-CM fraction recovered from the LV extracts of *Ido-1*^{-/-} mice (EC IDOKO) (n=3) and control littermates (n=7). One-way ANOVA was used followed by Tukey's multiple comparisons test. **C**, IDO activity (Kyn/Trp) in LV extracts of EC IDOKO mice (n=4) compared to their control littermates (EC IDO) (n=5), at day 1 after MI. **D-F**, Quantitative evaluation of left ventricle (LV) ejection fraction, LV systolic and diastolic volumes (**D**), infarct size (**E**) and interstitial fibrosis (**F**) of EC IDOKO mice compared to their control littermates (EC IDO) (n=10 per group), challenged with MI. **G**, Representative images and quantifications of TUNEL (terminal deoxynucleotidyl transferase-mediated dUTP nick end labeling) staining in the peri-infarcted area of the LV of EC IDOKO mice and control littermates (EC IDO) at day 2 post MI. Arrows point to apoptotic nuclei. Cardiac function and remodeling were evaluated at day 14 after MI. Representative images are presented. Mann Whitney test was used to compare EC IDO vs EC IDOKO groups. Individual data are presented as aligned dot plots, with the mean and s.e.m. **P*<0.05, ***P*<0.01, ****P*<0.001.

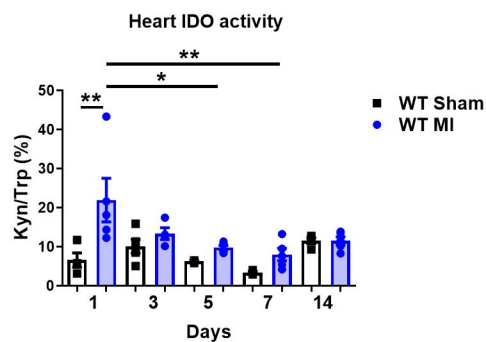
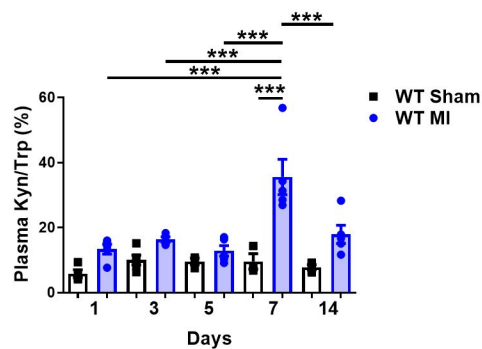
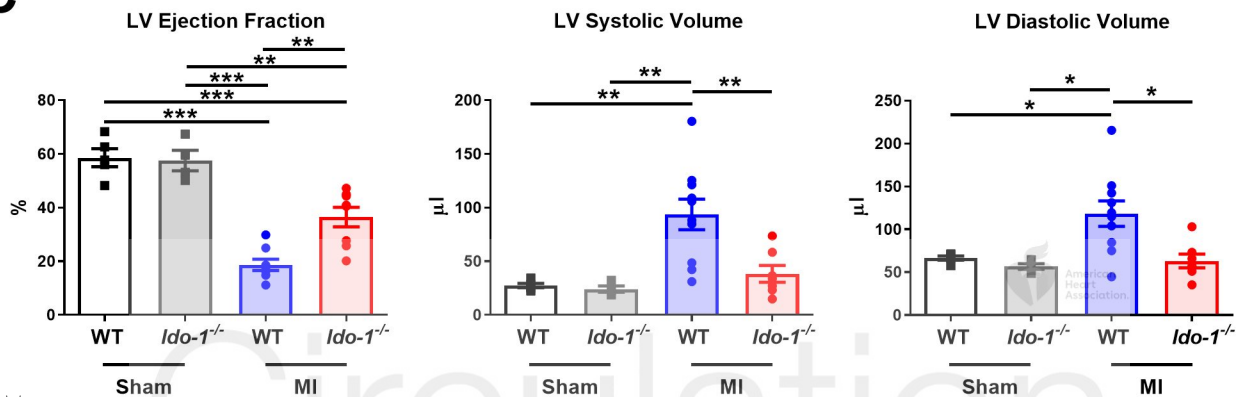
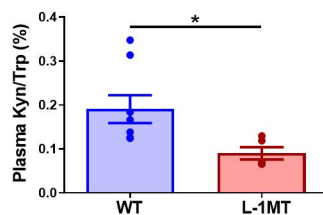
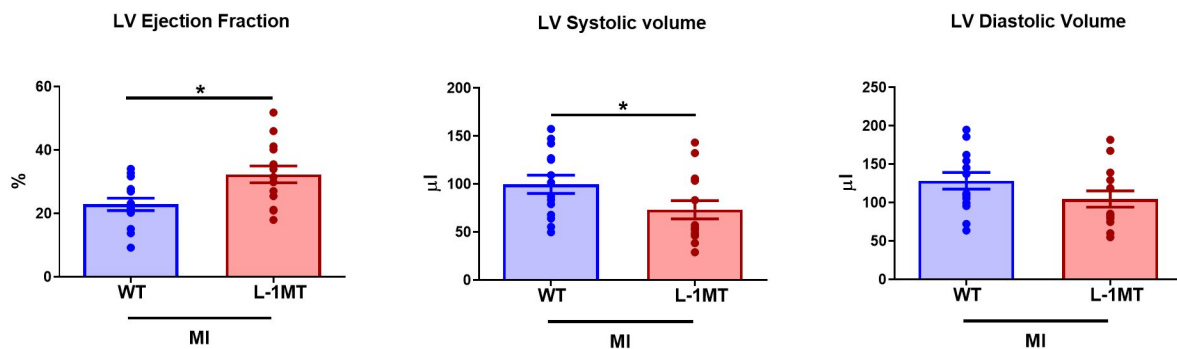
Figure 5. Kynurenine metabolite alters cardiac function and remodeling after MI

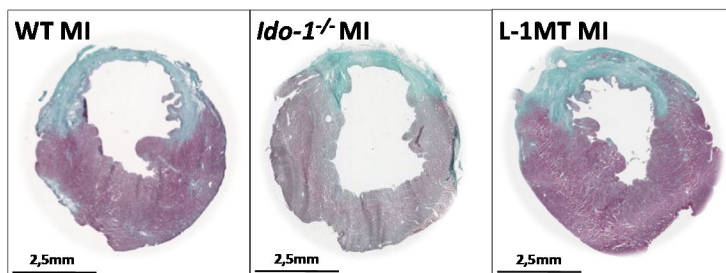
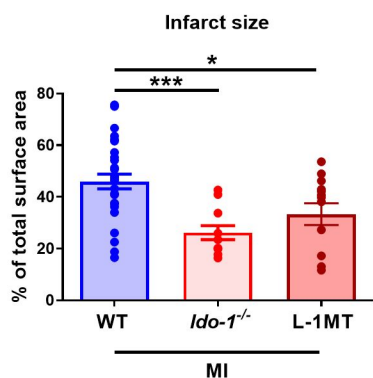
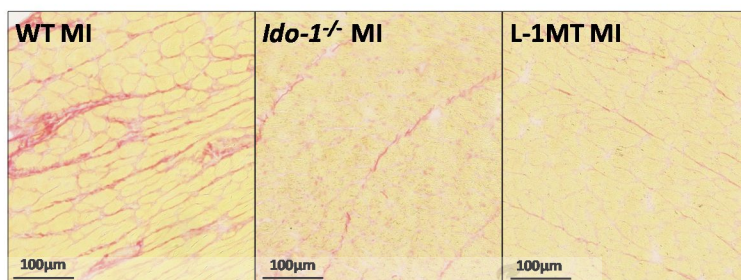
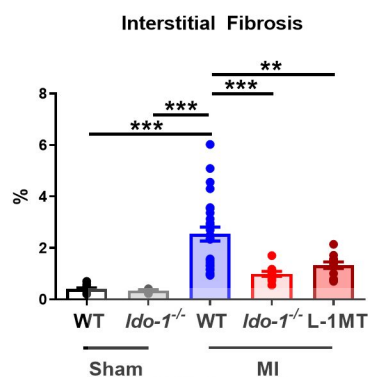
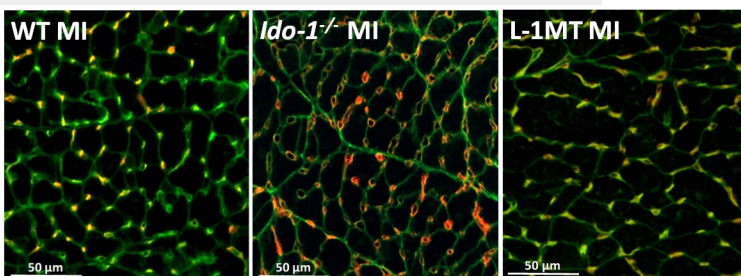
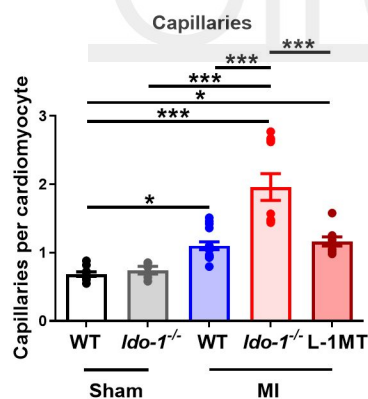
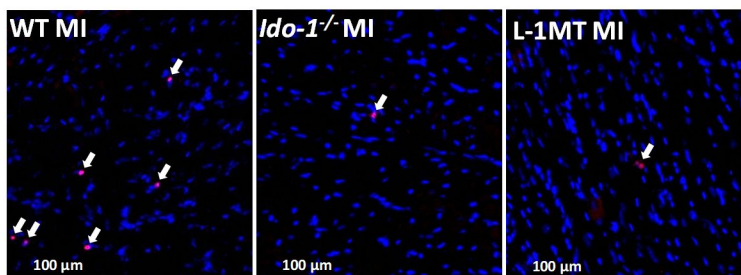
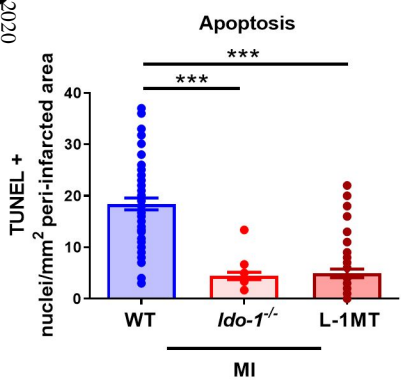
A-D, Kynurenine (Kyn) levels at day 3 after myocardial infarction (MI), left ventricle (LV) ejection fraction, LV systolic and diastolic volumes (**A**), capillary density (**B**), infarct size (**C**) and interstitial fibrosis (**D**) in *Ido-1*^{-/-} mice supplemented with Kyn (*Ido-1*^{-/-} + Kyn) (n= 9) compared to *Ido-1*^{-/-} mice (n=7), challenged with MI. **E**, TUNEL (terminal deoxynucleotidyl transferase-mediated dUTP nick end labeling) staining and quantification in the peri-infarcted area of the LV of *Ido-1*^{-/-} + Kyn mice compared to *Ido-1*^{-/-} at day 2 post MI. **F**, Representative images and quantification of reactive oxidative species (ROS) staining in cultured cardiomyocytes (CM) treated with either Kyn (10μM) or vehicle (DMSO, 1/3000), (n=4 wells per condition, the result shown is representative of 4 independent experiments). The pictures represent merged images of CM in green and ROS staining in red. ROS staining was normalized on CM area. Mann Whitney test was used to compare *Ido-1*^{-/-} vs *Ido-1*^{-/-} + Kyn and vehicle Kyn vs Kyn groups. **G**, TUNEL staining and quantification in the peri-infarcted area of the LV of *Ido-1*^{-/-} + Kyn mice compared to *Ido-1*^{-/-}, pre-treated with either aryl hydrocarbon receptor (AHR) antagonist (CH-223191) or its vehicle control (vehicle CH-223191), at day 2 post MI. Arrows point to apoptotic nuclei. Representative images are presented. One-way ANOVA was used followed by Tukey's multiple comparisons test. Cardiac function and remodeling were evaluated at day 14 after MI. Individual data are presented as aligned dot plots, with the mean and s.e.m. **P*<0.05, ***P*<0.01.

Figure 6. IDO specific deficiency in endothelial cell limits cardiomyocyte apoptosis and improves cardiomyocyte contractility.

A, Kynurenine (Kyn) levels in supernatants after 24-hours of culture of cardiomyocytes (CM) or non-cardiomyocytes (non-CM) isolated from the left ventricle (LV) of endothelial cell (EC) IDO deficient mice (EC IDOKO) and their control-matched animals, at day 1 after MI or either after sham condition (n= 3 per group). Two-way ANOVA was used followed by Tukey's multiple comparisons test. **B**, Representative images and quantification of TUNEL (terminal deoxynucleotidyl transferase-mediated dUTP nick end labeling) staining in cultured CM incubated with supernatants from cultured non-CM isolated from LV non-infarcted area of either EC IDOKO or their littermate controls challenged with MI or sham-operated mice (n=4 wells per condition, the result shown is representative of 2 independent experiments). Arrows point to apoptotic nuclei. Representative images are presented. One-way ANOVA was used followed by Tukey's multiple comparisons test. **C**, Representative images and quantification of ROS staining in the peri-infarcted area of EC IDOKO mice compared to their control littermates, at 14 days following MI. ROS staining area was normalized to the size of the peri-infarcted area. Arrows point to ROS staining. **D**, Contraction and relaxation velocities of isolated CM from EC IDOKO mice (n=3) compared to their control littermates (n=3), after 14 days post-MI. Each point represents a value of CM contractility. Mann Whitney test was used to compare EC IDO vs EC IDOKO groups. Individual data are presented as aligned dot plots, with the mean and s.e.m.

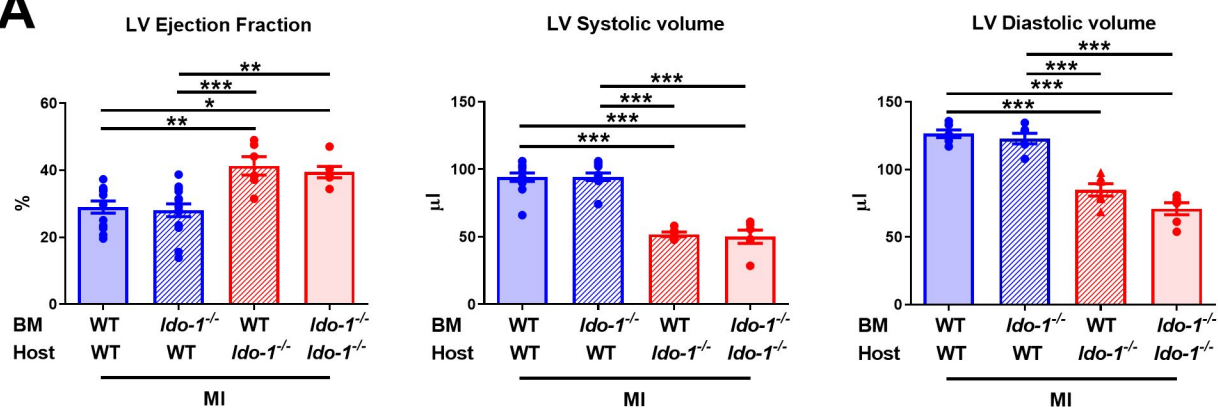
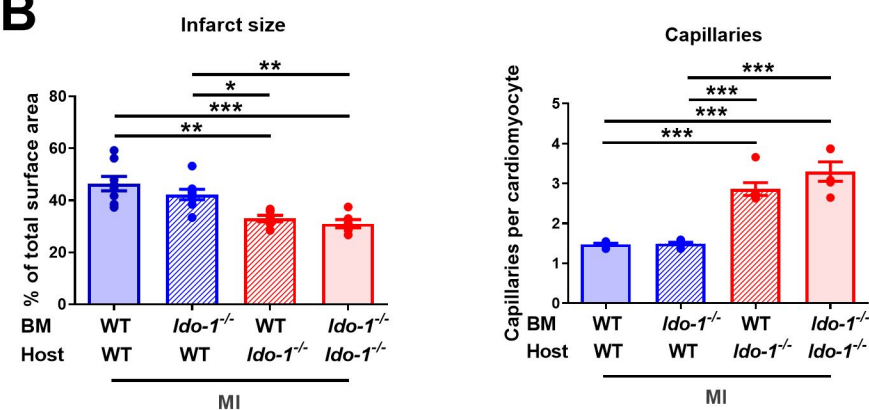
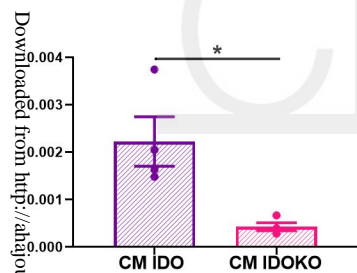
* $P < 0.05$, ** $P < 0.01$, *** $P < 0.001$.

A**B****C****D****E**

A**B****C****D**

Circulation

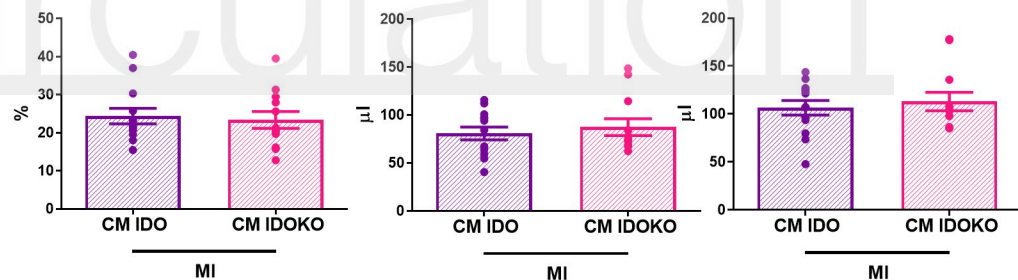
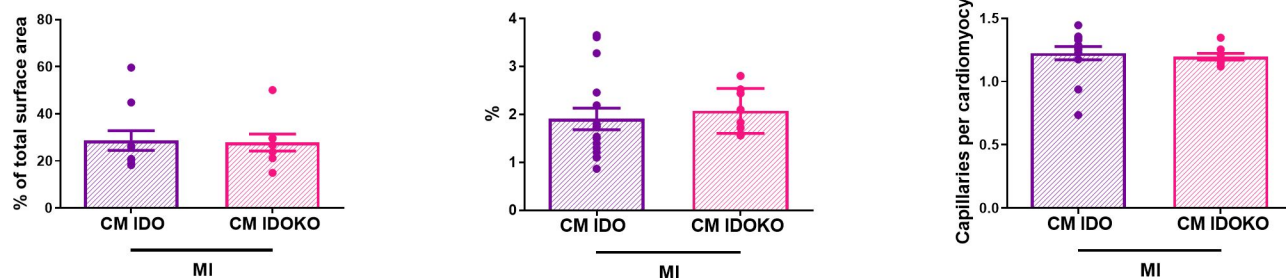
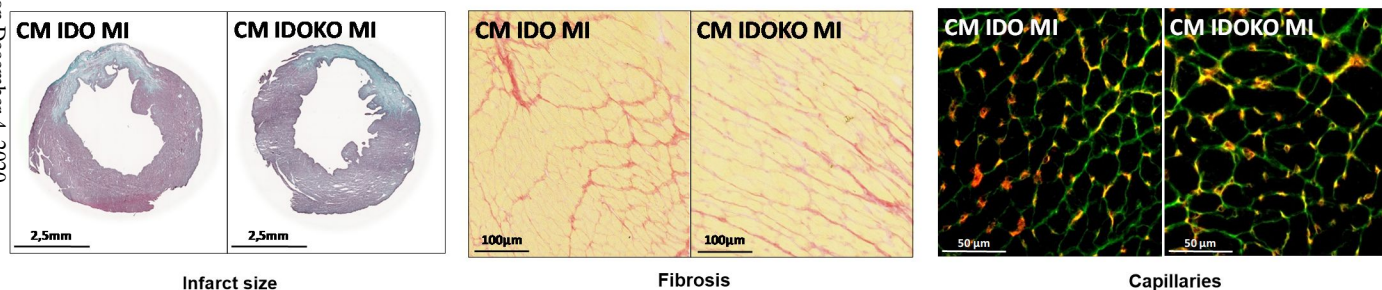
American Heart Association

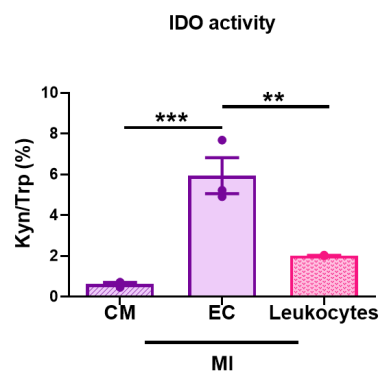
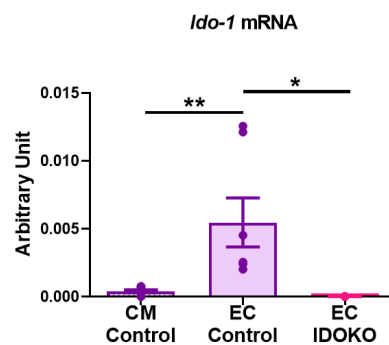
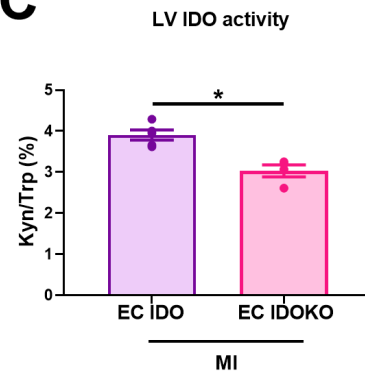
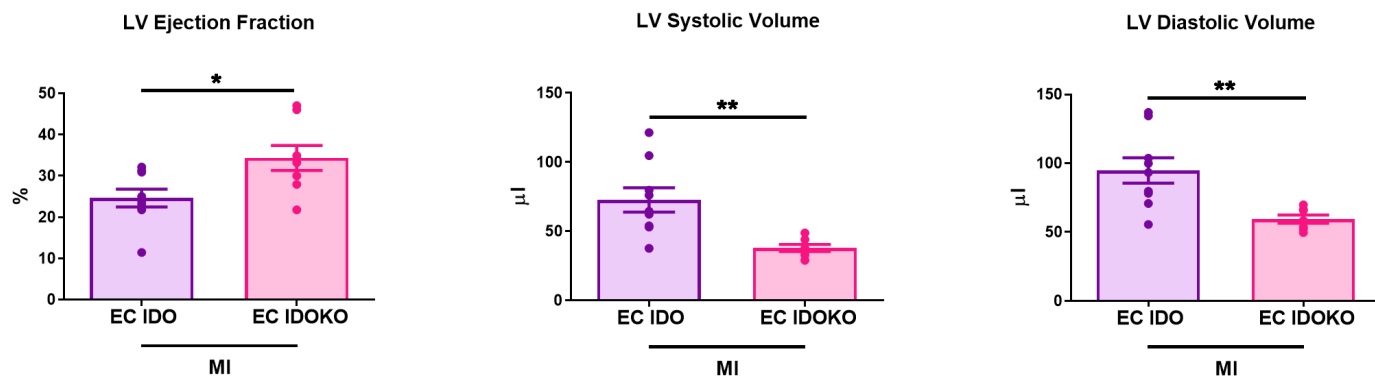
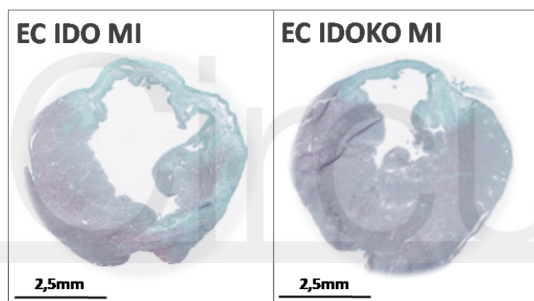
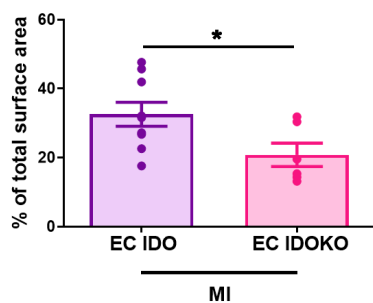
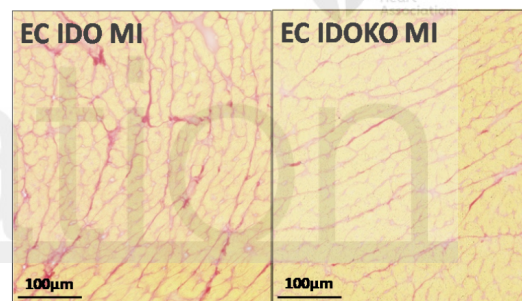
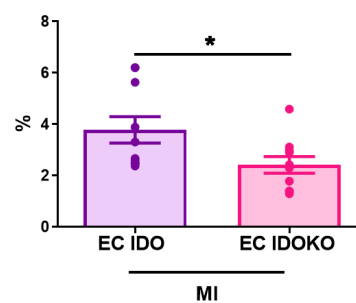
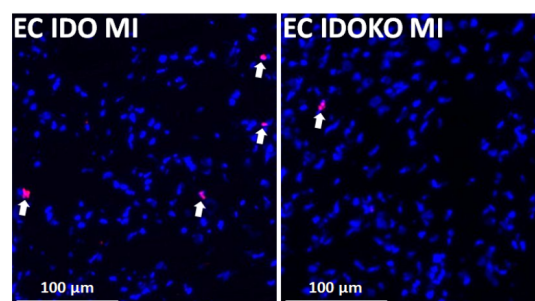
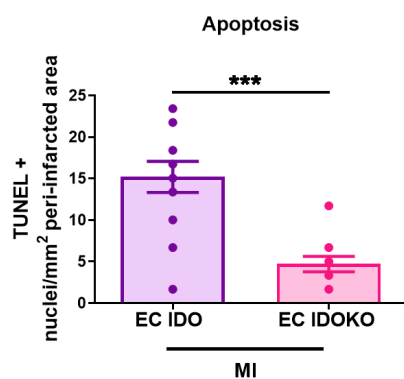
A**B****C**CM *Ido-1* mRNA**D**

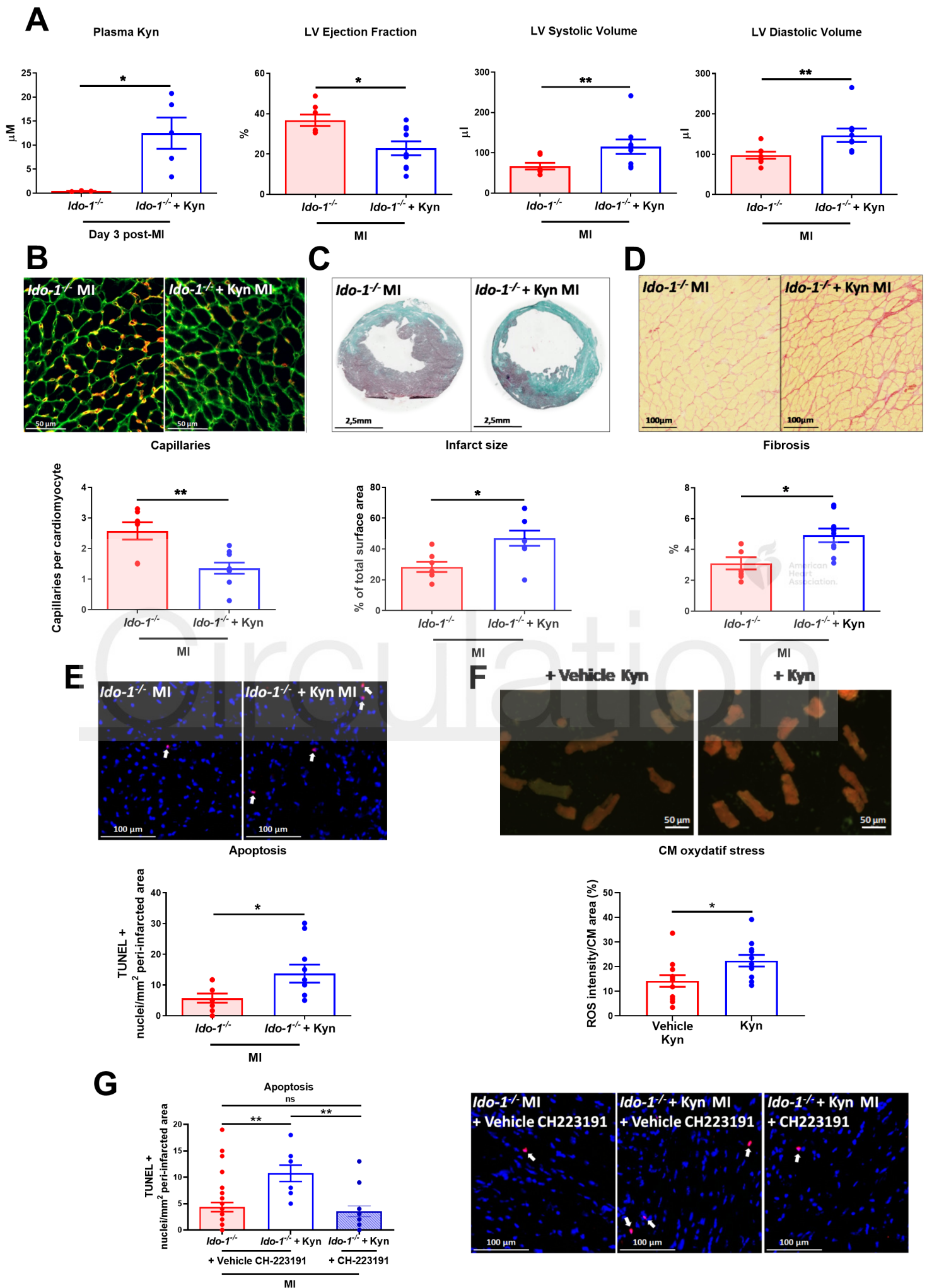
LV Ejection Fraction

LV Systolic Volume

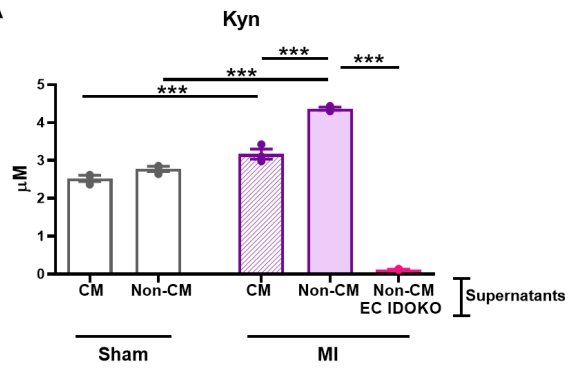
LV Diastolic Volume

**E**

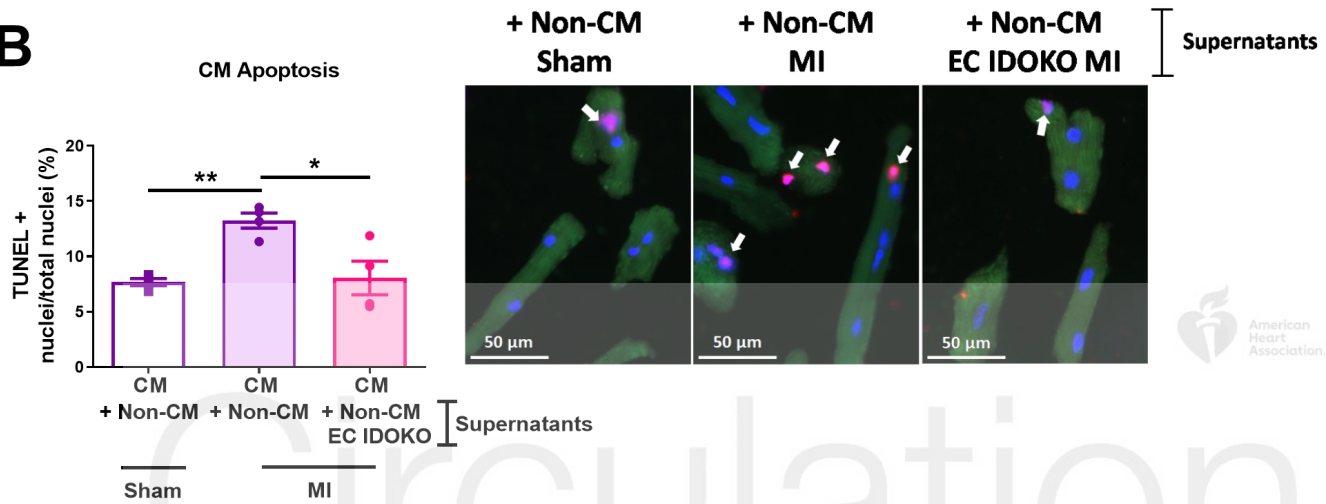
A**B****C****D****E****Infarct size****F****Fibrosis****G**



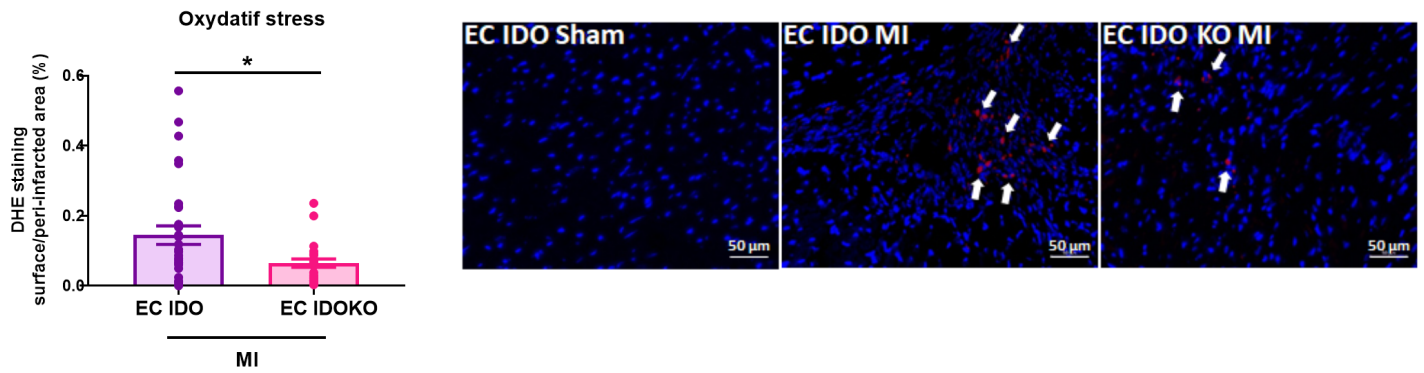
A



B



C



D

